

# DAMAGE SUPPRESSION IN UD-CFRP WITH FIBRE DISCONTINUITY BY INTERLAMINAR TOUGHENING USING POLYAMIDE MESH

Hayato Nakatani<sup>1</sup>, Tatsuya Imamura<sup>2</sup> and Katsuhiko Osaka<sup>3</sup>

<sup>1</sup>Department of Mechanical & Physical Engineering, Osaka City University,  
3-3-138 Sugimoto, Sumiyoshi, Osaka, Japan

Email: hayatonakatani@imat.eng.osaka-cu.ac.jp, Web Page: <http://www.osaka-cu.ac.jp/en>

<sup>2</sup>Master's Student, Department of Mechanical & Physical Engineering, Osaka City University, Japan

<sup>3</sup> Department of Mechanical & Physical Engineering, Osaka City University, Japan

**Keywords:** Unidirectional Laminates, Fibre Discontinuity, Interlaminar Crack, Polyamide Mesh, Fracture Toughness

## Abstract

A fiber discontinuity in fibre reinforced composite laminates may act as a source of stress concentration that induces damage onset. A mesh made of thermoplastic polyamide (PA) as an interlayer is inserted between fiber continuous and discontinuous plies in order to suppress an interlaminar cracking in unidirectional CFRP laminates that contain fiber discontinuity at the centre of the laminates. It is experimentally shown that by inserting PA mesh the onset stress of the interlaminar crack increased significantly. The stabilized end notched flexure (ENF) tests using strain gages are carried out to obtain a continuous R-curve of the mode II interlaminar fracture toughness  $G_{II}$ . By inserting the PA mesh  $G_{II}$  for initial crack growth  $G_{IIC} = 1.60 \text{ kJ/m}^2$  and for during crack propagation  $G_{IIR} = 3.82 \text{ kJ/m}^2$  can be achieved. It is also indicated that an analytical model suggested here that incorporates energy release rate during the interlaminar crack growth can predict the stress of the interlaminar crack onset for different number of discontinuous plies by applying  $G_{IIR}$  not  $G_{IIC}$  for both the laminates with and without PA mesh.

## 1. Introduction

Carbon fibre reinforced composites such as CFRPs recently have been applied to not only aerospace but also automobile structures due to their high specific strength and stiffness. Because of their fibre direction dependent properties, continuous fibres should be oriented in the same direction with the predicted load direction in structural designs. When one fabricates complex composite geometries by laminating unidirectional prepregs, for example, some precuts or slits are introduced to them to achieve appropriate fibre directions and also to trace the shape without wrinkles. It is significant for wide application of CFRP to understand the strength and damage behaviour in the CFRP laminates containing fibre discontinuities introduced by prepreg cuttings.

To date, effect of the prepreg cuttings in tapered composite structures on their mechanical properties and damage behaviour has been evaluated to some extent. For instance, Fish and Lee predicted delamination onset stress in the structure based on maximum shear stress criteria [1]. Her represented the ply drop-off part where delamination and fracture can be easily taken place by a finite element model, and attempted to analyse the singular stress field in that part [2]. Taketa et al. successfully fabricate complexly shaped composite components with layered structure maintained by using sheets made by introducing slits into a conventional prepreg [3]. Most of these reports, however, dealt with

the multiple fibre discontinuity parts and/or off-axis loading since they assumed the fibre discontinuity in real structures. Nakatani et al. have evaluated relations between mechanical properties and damage behaviour and predicted damage onset stress by an analytical model for unidirectional CFRP laminates  $[0_8]$  containing fibre discontinuities in 2, 4 and 6 plies that locates in centre of the laminate [4, 5]. They revealed that two main damage modes were observed under tensile loading; a crack initiated in the resin rich part that is formed at the edge of fibre discontinuity then this crack proceeded into interlaminar between the continuous and discontinuous plies.

In this study, a mesh made of thermoplastic polyamide (PA) is inserted between fibre continuous and discontinuous plies as an interlayer to suppress the interlaminar cracking as the second damage mode. It is expected that one can achieve the crack suppression that can be observed in the interlaminar-toughened CFRP laminates at a relatively low cost. Here, the increases of onset stress of the interlaminar cracking between fibre continuous and discontinuous plies are experimentally presented, and is also evaluated in terms of interlaminar fracture toughness and analytical prediction.

## 2. Materials used and experimental procedures

Unidirectional CFRP laminates were fabricated using 8 plies of carbon/epoxy prepregs (T700SC/2592, Toray) with an autoclave. The fibre discontinuities were introduced by placing prepregs, that were pre-cut perpendicular to the fiber direction, edge to edge while making clearance gaps as narrow as possible before moulding. Fibre discontinuities were formed in 2, 4 and 6 plies out of 8 plies in the centre of laminates, then PA mesh were inserted between fibre continuous and discontinuous plies as shown in Fig. 1(a). The unidirectional CFRP laminates without PA mesh were also tested for comparison. In Fig. 1(b) one can see appearance of the PA mesh (fibre diameter:  $50\mu\text{m}$ , thickness:  $87\mu\text{m}$ , opening:  $95\mu\text{m}$ , N-NO175T, NBC Meshtec Inc.).

After the autoclave moulding the unidirectional CFRP laminates were cut into  $200\text{ mm} \times 10\text{ mm}$  coupons then GFRP tabs were adhered both ends for gripping and strain gages were attached on just above the fibre discontinuity and also on the position 20 mm away from the fibre discontinuity to obtain tensile specimens as shown in Fig. 2. Tensile tests were carried out using a universal load frame (Autograph AG-1, Shimadzu Corp.) under crosshead speed of 1 mm/min. During the tensile testing an optical video microscope was applied to observe damage initiation and growth that can be seen in the edge surface of the specimen.

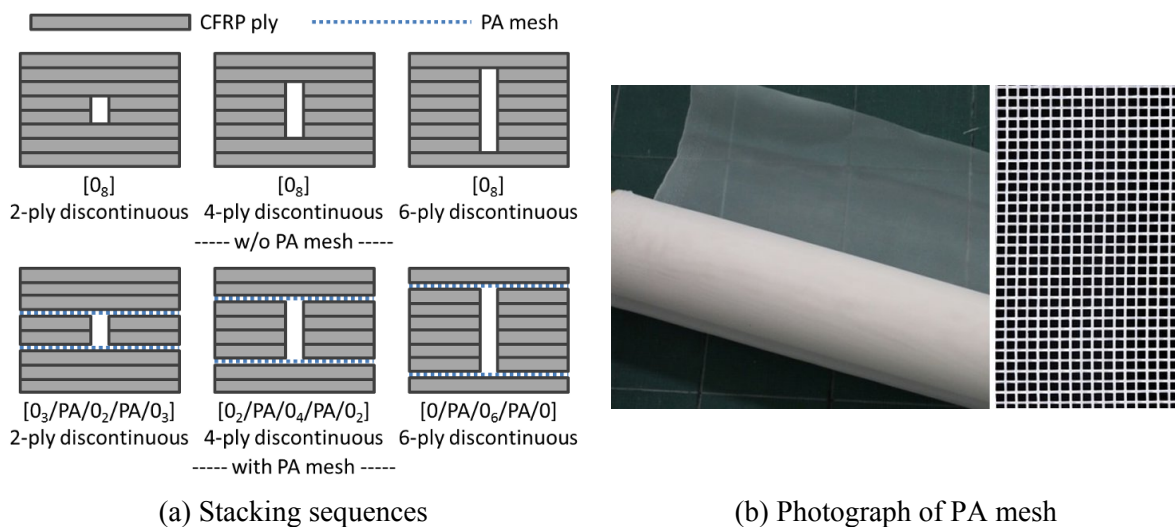


**Figure 1.** The unidirectional CFRP laminates with fibre discontinuity and PA mesh inserted.

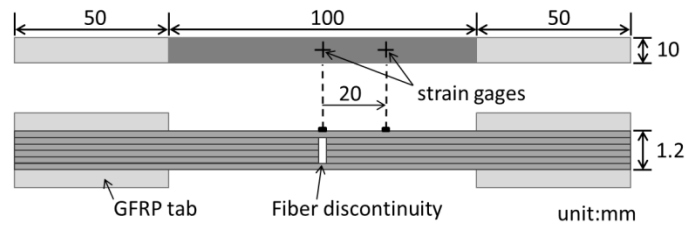


**Figure 2.** Schematic of the unidirectional CFRP laminates with fibre discontinuity.

### 3. Experimental results and discussions

#### 3.1. Stress-strain relations and damage behaviour

Stress-strain curves for the CFRP laminates containing fibre discontinuity are shown in Fig. 3. As for the laminates without PA mesh (Fig. 3(a)), one can see non-linear stress-strain relations just above the fibre discontinuity that are represented by solid lines until certain stress levels. Previous works have found that these non-linear responses correspond to initiation of crack in the resin rich region at the edge of fibre discontinuity. For the specimens with PA mesh the same can be said; the initial bend or non-linear behaviour for the stress-strain curves just above the fibre discontinuity as shown in Fig. 3(b) should be related to the crack initiation in the resin rich region. From microscopic observation of edge surface of the 4-ply discontinuous specimen, one can see the crack in the resin rich region under the stress of 700 MPa regardless of whether the PA mesh is inserted (Fig. 4(a)). It should be noted that suppression of this crack by inserting the PA mesh is not expected here.

As for the stress-strain relations 20 mm away from the fibre discontinuity that are represented by dashed line, one can see discontinuous behaviours where strain increased sharply after linear responses for the laminates without PA mesh. These discontinuous responses have already found to be attributed to the onset of interlaminar crack between fibre continuous and discontinuous plies. So the interlaminar crack onset that is interested in this paper can be detected by these discontinuous responses or the sharp increase in the strain 20 mm away from fibre discontinuity. Fig. 4(b) shows microscopic observation results of the 4-ply discontinuous specimen right after the sharp increase of the strain. One can see that the crack which is initiated in the resin rich region proceeded into the interlaminar between fibre continuous and discontinuous plies. Compared to this, stress of discontinuous responses in the stress-strain curves i.e. the interlaminar crack onset increased significantly or disappeared by inserting the PA mesh. Microscopic observation of 4-ply discontinuous specimen with PA mesh also revealed that the interlaminar crack was not induced even if the tensile

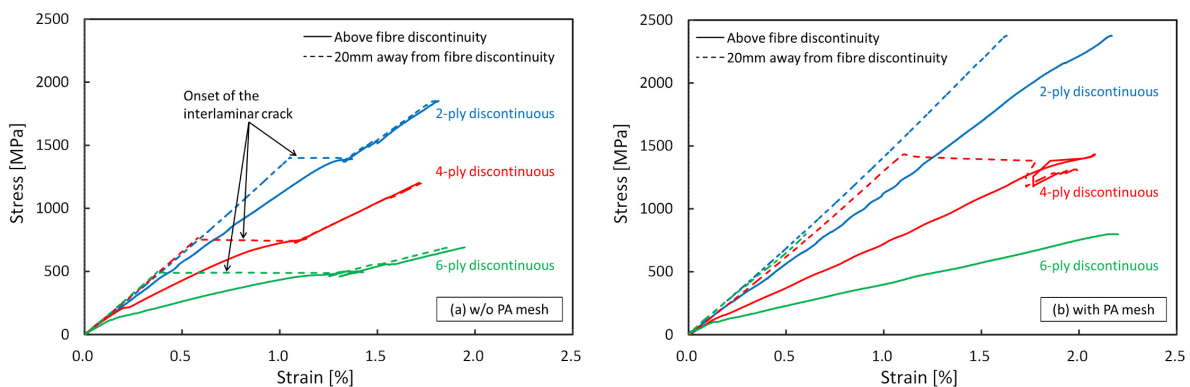


**Figure 3.** Stress-strain curves of the unidirectional CFRP laminates containing fibre discontinuity.

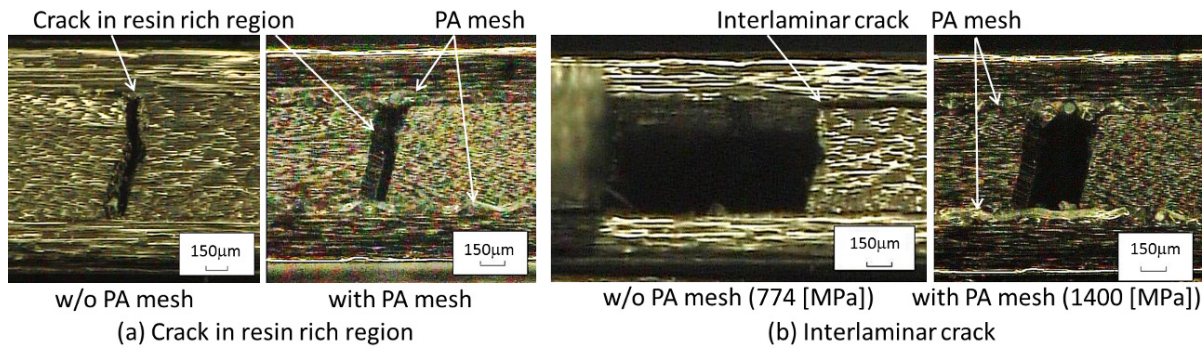


**Figure 4.** Microscopic observation of cracks near the fibre discontinuity.

stress of 1400 MPa was applied as shown in Fig. 4(b). Since some specimens did not show the onset of interlaminar crack it seems that the crack onset stress is comparable with the fracture stress of the laminates.

### 3.2. Stabilized End Notched Flexure (ENF) tests by strain measurement

The interlaminar crack growth should depend on the mode II interlaminar fracture toughness between the fibre continuous and discontinuous plies. According to Ref. [6] an end notched flexure (ENF) tests with a control method to stabilize the crack propagation using long and short strain gages attached on the back surface (tensile side during the three point bending) of the specimen are conducted to obtain relations of crack extension  $\Delta a$  and interlaminar fracture toughness in mode II ( $G_{II}$ ) also known as the crack growth resistance curve, R-curve.

Specimens for the stabilized ENF testing are unidirectional carbon/epoxy laminates of  $[0_{12}/0_{12}]$  (without PA mesh) and  $[0_{12}/PA/0_{12}]$  (PA mesh inserted) with initial crack introduced before testing. Here specimen width  $B$  and thickness  $2h$  were 20 mm and 3.0-3.4 mm, respectively. Two strain gages with gage length of 30 mm and 5 mm were attached on the back surface of the laminates as shown in Fig. 5. The long gage was positioned so as to cover both the edge of the initial crack and loading point, and the location of the short gage should satisfy following relation,

$$s = l - (r + 4) \quad (1)$$

where  $s$  and  $r$  are distances between supporting point and centre of the short gage, and loading point and center of the long gage, respectively. Displacement of the cross-head of the testing frame was controlled to obtain a constant increase rate of difference in outputs of the two strain gages. Based on relations between strain distribution in the gage part and crack length, and strain energy stored in the specimen obtained by the elementary beam theory, the mode II interlaminar fracture toughness  $G_{II}$  can be given as,

$$G_{II} = 4g^2 E h \varepsilon_f^2 \frac{a^2}{(a^2 + \alpha)^2} \quad (2)$$

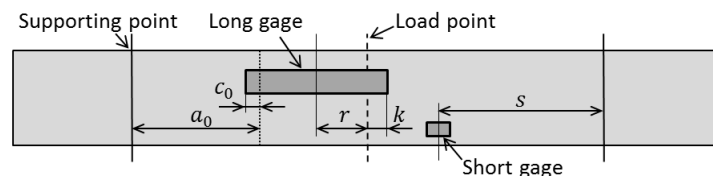


**Figure 5.** Location of the long and short strain gages for stabilized ENF test.

where  $E$  is bending stiffness and  $g$  is gage length of the long gage (=30mm).  $\varepsilon_f$  is difference between strain outputs of the two gages during the crack propagation as,

$$\varepsilon_f = \varepsilon_g - \varepsilon_s = \frac{3P}{8gEBh^2} (a^2 - 2a_0^2 + 4a_0c_0 - 2c_0^2 + l^2 + 2kl - k^2) - \frac{3Ps}{4EBh^2} \quad (3)$$

where  $a_0$  is the initial crack length,  $k$  and  $l$  are distances between loading point and edge of the long gage, and between supporting and loading points, respectively.  $c_0$  as the overlapped length of the long gage and initial crack can be given by

$$c_0 = a_0 - \sqrt{\frac{1}{2} \left( a_0^2 + 2kl - k^2 + l^2 - 2gs - \frac{8gEBh^2}{3P_{nl}} \varepsilon_{f_{nl}} \right)}. \quad (4)$$

$P_{nl}$  and  $\varepsilon_{f_{nl}}$  denote load and difference in strain output at the point where the load-strain curve starts to show non-linearity. With the  $c_0$ , the crack length  $a$  during the crack propagation can be obtained by using load  $P$  and difference in strain strain output  $\varepsilon_f$  as,

$$a^2 = (2a_0^2 - 4a_0c_0 + 2c_0^2 - l^2 - 2kl + k^2 + 2gs) + \frac{8gEBh^2}{3P} \varepsilon_f. \quad (5)$$

The constant term  $\alpha$  in Eq. (2) is given by

$$\alpha = -2a_0^2 + 4a_0c_0 - 2c_0^2 + l^2 + 2kl - k^2 - 2gs. \quad (6)$$

Fig. 6 shows the R-curve obtained by the stabilized ENF tests for the laminates with and without PA mesh. It should be noted that the mode II interlaminar fracture toughness during the crack propagation  $G_{IIR}$  is remarkably improved by inserting PA mesh. Here range of crack extension  $\Delta a$  from 5 mm to 20 mm was taken, and averaged  $G_{II}$  in this range was adopted as  $G_{IIR}$  as shown in Table 1. The critical interlaminar fracture toughness for initial crack growth in mode II  $G_{IIC}$  obtained by standard ENF tests (JIS K7086 in Japan) are also shown in the table. One can see that by inserting PA mesh higher values of both  $G_{IIC}$  and  $G_{IIR}$  are achieved compared to the laminates without PA mesh, and increase in  $G_{IIR}$  was significant. Fig. 7 shows fracture surface of the specimen after ENF tests. It is observed that the interlaminar crack propagated between the one side of the PA mesh and the CFRP ply by tearing off the epoxy resin that was filled in opening of the mesh. Large area of interface between the PA mesh

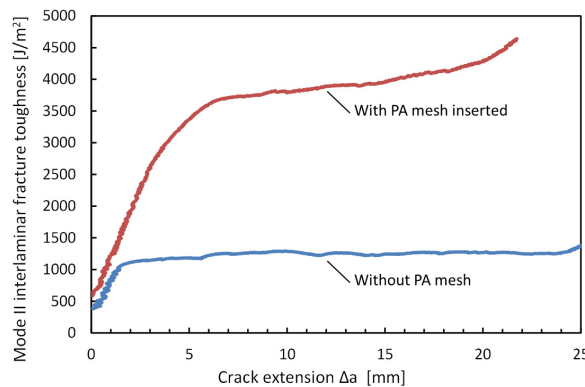


**Figure 6.** Crack growth resistance curve (R-curve) for mode II.

**Table 1.** Interlaminar fracture toughness in mode II obtained by the stabilized ENF tests.

	$G_{IIC}$ [kJ/m <sup>2</sup> ]	$G_{IIR}$ [kJ/m <sup>2</sup> ]
w/o PA mesh	1.11	1.23
PA mesh inserted	1.60	3.82

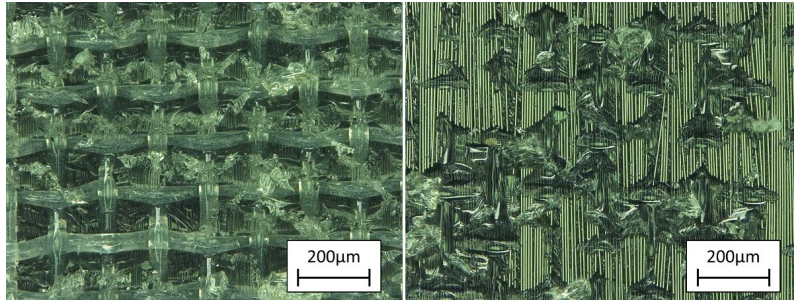


**Figure 7.** Fracture surface of the specimen after the stabilized ENF test.

and epoxy resin that show debonding as interlaminar crack can enable strain energy to be released without rapid crack growth, then apparent mode II interlaminar fracture toughness can be improved.

#### 4. Prediction of interlaminar crack onset stress

##### 4.1. Analytical model

An analytical model that calculates energy release rate by considering force equilibrium before and after the onset of the interlaminar crack is proposed to see if the model can predict the onset stress by applying mode II interlaminar fracture toughness even if the PA mesh is inserted to the CFRP laminates. As shown in Fig. 8 a quarter of the laminate was modeled in 2-dimension. The crack in the resin rich region and the interlaminar crack with its length of  $a$  as red dashed line are already presented. Shaded part is assumed not to be subjected to load since this part is surrounded by the cracks.  $E_1$ ,  $E_2$ ,  $t_1$  and  $t_2$  are the elastic moduli and thicknesses of the fibre continuous and discontinuous plies, respectively. Here  $E_1 = E_2 = 130$  GPa and  $t_1 = t_2 = 0.6$  mm. For  $0 < x < a$  and  $a < x < L$ , which are subscripted as "i" and "ii" respectively, strains  $\varepsilon_i$  and  $\varepsilon_{ii}$  can be written as

$$\varepsilon_i = \frac{\sigma_i}{E_i} = \frac{P}{E_1 t_1} \quad (7)$$

$$\varepsilon_{ii} = \frac{\sigma_{ii}}{E_{ii}} = \frac{P}{E_1 t_1 + E_2 t_2} = \frac{P}{E_1 (t_1 + t_2)} \quad (8)$$

where  $P$  is load. Displacement in entire model  $\delta$  under load  $P(a)$  is then,

$$\delta = \varepsilon_i a + \varepsilon_{ii} (L - a) = \frac{t_1 L + t_2 a}{E_1 t_1 (t_1 + t_2)} P(a) . \quad (9)$$

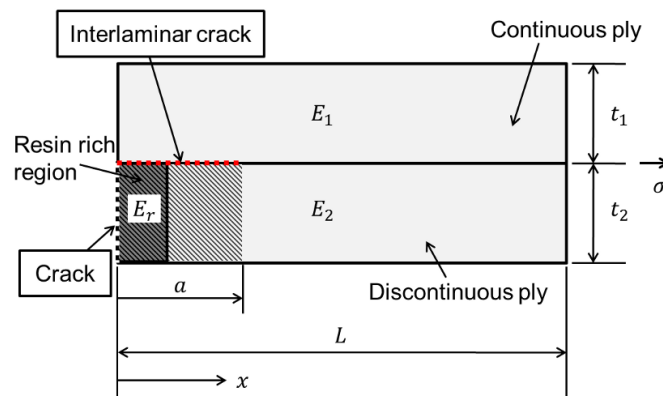


**Figure 8.** Analytical model to predict the interlaminar crack onset stress.

The load  $P(a)$  can be given as a function of the interlaminar crack length  $a$  as,

$$P(a) = \frac{E_1 t_1 (t_1 + t_2)}{t_1 L + t_2 a} \delta . \quad (10)$$

By the increase of crack length from  $a$  to  $a+da$  at the moment the load reaches  $P(a)$  during the tensile loading, the load is assumed to decrease to  $P(a+da)$  under constant displacement. Change in potential energy  $d\Pi$  by this interlaminar crack growth can be expressed as,

$$d\Pi = \frac{\delta^2}{2} \left( \frac{1}{C(a+da)} - \frac{1}{C(a)} \right) \quad (11)$$

where  $C(a)$  is the compliance defined as,

$$C(a) \equiv \frac{\delta}{P(a)} = \frac{t_1 L + t_2 a}{E_1 t_1 (t_1 + t_2)} . \quad (12)$$

Now one can obtain the energy release rate  $\mathcal{G}$  by the interlaminar crack growth as

$$\mathcal{G} = - \lim_{da \rightarrow 0} \frac{d\Pi}{da} = - \frac{\delta^2}{2} \frac{d}{da} \left( \frac{1}{C(a)} \right) = \frac{\sigma^2 (t_1 + t_2) t_2}{2E_1 t_1} \quad (13)$$

where  $\sigma$  is applied stress. From Eq. (13) the stress for the crack growth  $\sigma_0$  can be given as,

$$\sigma_0 = \sqrt{\frac{2E_1 t_1}{t_2 (t_1 + t_2)} \mathcal{G}_c} \quad (14)$$

where  $\mathcal{G}_c$  is critical energy release rate. Since it was observed that onset of the interlaminar crack corresponds to propagation of the crack originated in the resin rich region, the stress of crack growth of Eq. (14) can be compared to the experimental onset stress of the crack.

#### 4.2. Predicted stress of the interlaminar crack onset

By applying mode II interlaminar fracture toughness  $G_{II}$  shown in Table 1 to the critical energy release rate  $\mathcal{G}_c$  in Eq. (14) one can predict relations between the onset stress of the interlaminar crack and number of discontinuous plies out of 8 plies as shown in Fig. 9. Symbols denote the experimental results for the stresses of the discontinuous responses in stress-strain relations as the interlaminar crack onset. For the specimens that did not show the interlaminar crack by inserting PA mesh their fracture stresses are adopted here. Predicted stress agreed well with the experimental results for both the laminates without and with PA mesh when the mode II interlaminar fracture toughness during crack propagation  $G_{IIR}$  is adopted as depicted as solid curves. Compared to this, onset stresses predicted by using  $G_{IIC}$  (dotted line in Fig. 9) are much lower than the experimental results especially for the

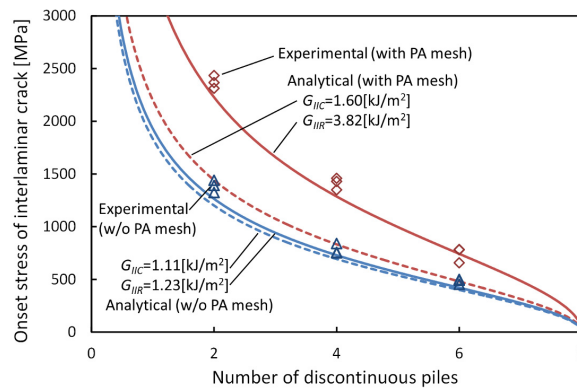


**Figure 9.** Predicted interlaminar crack onset stress compared to the experimental results.

laminate with the PA mesh inserted.

Onset stress of the interlaminar crack here is defined by the sharp increase of the strain detected by strain gage which is located 20 mm away from the fibre discontinuity on the specimen surface. So as to be detected by the strain gage, the interlaminar crack should proceed 20 mm between fibre discontinuous and continuous plies. Hence the fracture toughness during the crack propagation  $G_{IIR}$ , not the  $G_{IIC}$  for initial crack growth, can represent comparable fracture behaviour similar to that evaluated in the experiments.

## 5. Conclusions

To suppress growth of the interlaminar crack between the fibre continuous and discontinuous plies in the unidirectional CFRP laminates those contain fibre discontinuities, the mesh of thermoplastic polyamide (PA) was inserted as an interlayer. It is experimentally shown by tensile testing that a sharp increase in strain at 20 mm away from the fibre discontinuity which corresponds to the interlaminar crack onset can be seen at higher stress level or does not occur until rupture of the laminate by inserting the PA mesh. The stabilized end notched flexure (ENF) tests by strain measurement was carried out to obtain the crack growth resistance curve, a.k.a. R-curve, in mode II. It is demonstrated that mode II interlaminar fracture toughness for initial crack growth  $G_{IIC}=1.60$  kJ/m<sup>2</sup> and during crack propagation  $G_{IIR}=3.82$  kJ/m<sup>2</sup> was achieved. These should be compared to  $G_{IIC}=1.11$  kJ/m<sup>2</sup> and  $G_{IIR}=1.23$  kJ/m<sup>2</sup> without PA mesh. An analytical model that incorporates energy release rate by the interlaminar crack growth was suggested to predict the crack onset stress. The model successfully predicted the crack onset stress when the  $G_{IIR}$  was adopted for calculation for both the laminates with and without PA mesh since the crack should proceed some distance to be detected by the strain gage.

## Acknowledgments

Authors are grateful for Prof. Ogihara of Tokyo University of Science (Japan) for providing valuable advices for the prediction using the analytical model.

## References

- [1] J.C. Fish and S.W. Lee. Delamination of tapered composite structures. *Engineering Fracture Mechanics*, 34:43-54, 1989.
- [2] S.-C. Her. Stress analysis of ply drop-off in composite structures. *Composite Structures*, 57:235-244, 2002.
- [3] I. Taketa, T. Okabe and A. Kitano. A new compression-molding approach using unidirectionally arrayed chopped strands. *Composites: Part A*, 39:1884-1890, 2008.
- [4] H. Nakatani, K. Nakaya, A. Matsuba, Y. Kouno and S. Ogihara. Effect of prepreg cut on the mechanical properties in CFRP laminates. *Journal of Solid Mechanics and Materials Engineering*, 5(12):742-752, 2011.
- [5] H. Nakatani, K. Nakaya, A. Matsuba, Y. Kouno and S. Ogihara. Damage behavior in unidirectional CFRP laminates with fiber discontinuity. *Transactions of the Japan Society of Mechanical Engineers Series A* (in Japanese), 79(799):294-303, 2013.
- [6] K. Katsura, K. Tanaka and K. Aono. Precise instrumentation and stabilization of interlaminar fracture toughness test on CFRP by long gage strain measurement. *Transactions of the Japan Society of Mechanical Engineers Series A* (in Japanese), 65(634):1405-1411, 1999.